

# Investigation of dark matter-dark energy interaction cosmological model

J. S. Wang<sup>1,2</sup> and F. Y. Wang<sup>1,2</sup>

<sup>1</sup> School of Astronomy and Space Science, Nanjing University, Nanjing 210093, China;

<sup>2</sup> Key Laboratory of Modern Astronomy and Astrophysics (Nanjing University), Ministry of Education, Nanjing 210093, China

Preprint online version: October 16, 2018

## ABSTRACT

In this paper, we test the dark matter-dark energy interacting cosmological model with a dynamic equation of state  $w_{DE}(z) = w_0 + w_1 z/(1+z)$ , using type Ia supernovae (SNe Ia), Hubble parameter data, baryonic acoustic oscillation (BAO) measurements, and the cosmic microwave background (CMB) observation. This interacting cosmological model has not been studied before. The best-fitted parameters with  $1\sigma$  uncertainties are  $\delta = -0.022 \pm 0.006$ ,  $\Omega_{DM}^0 = 0.213 \pm 0.008$ ,  $w_0 = -1.210 \pm 0.033$  and  $w_1 = 0.872 \pm 0.072$  with  $\chi_{min}^2/dof = 0.990$ . At the  $1\sigma$  confidence level, we find  $\delta < 0$ , which means that the energy transfer prefers from dark matter to dark energy. We also find that the SNe Ia are in tension with the combination of CMB, BAO and Hubble parameter data. The evolution of  $\rho_{DM}/\rho_{DE}$  indicates that this interacting model is a good approach to solve the coincidence problem, because the  $\rho_{DE}$  decrease with scale factor  $a$ . The transition redshift is  $z_{tr} = 0.63 \pm 0.07$  in this model.

**Key words.** dark energy-cosmological parameters-cosmology: observations

## 1. Introduction

Recent observations with increasing accuracy show that the universe is undergoing an accelerating expansion, such as type Ia supernovae (SNe Ia; Riess et al. 1998; Perlmutter et al. 1999; Suzuki et al. 2012), cosmic microwave background (CMB) from Wilkinson Microwave Anisotropy Probe 9 years (WMAP9; Hinshaw et al. 2013) and Planck (Planck Collaboration et al. 2013), the baryonic acoustic oscillation (BAO) from 6dF Galaxy Redshift Survey (6dFGRS; Beutler et al. 2011), the Sloan Digital Sky Survey (SDSS; Eisenstein et al. 2005; Percival et al. 2010; Anderson et al. 2012), WiggleZ (Blake et al. 2012) and so on. Planck results also confirm that the universe is spatially flat, in other words, the curvature parameter  $\Omega_K$  is  $-0.0000^{+0.0066}_{-0.0067}$  (Planck Collaboration et al. 2013) at 95% confidence level. The main components of the universe are dark matter (DM) and dark energy (DE). The special characteristic of DE is negative pressure. The simplest candidate of DE is the cosmological constant with equation of state (EoS)  $w = p_\Lambda/\rho_\Lambda = -1$ . However, there are some problems with the  $\Lambda$ CDM model. The most important one is coincidence problem, which says why the DE density is comparable with the matter density at present. Yet, the energy density of DE is non-dynamical while matter density decreases with  $a^{-3}$ , where  $a = 1/(1+z)$  is scale factor.

In order to solve the coincidence problem, many methods have been proposed (Ratra & Peebles 1988; Caldwell 2002; Armendariz-Picon, Mukhanov & Steinhardt 2001; Feng, Wang & Zhang 2005). The interacting dark sectors models are possible solutions, which means there is energy exchanges between DE and DM. So the energy density ratio  $\rho_{DM}/\rho_{DE}$  can decrease slower than  $a^{-3}$ . We consider that the energy exchanges through a interaction term  $Q$ . The conservation of the total stress-energy tensor, and a scalar-field model of

dark energy is also assumed in this case

$$(\dot{\rho}_B + \dot{\rho}_{DM}) + 3H(\rho_B + \rho_{DM}) = -Q, \quad (1)$$

$$\dot{\rho}_{DE} + 3H\rho_{DE}(1 + w_{DE}) = Q, \quad (2)$$

where  $\rho_B$  and  $\rho_{DM}$  represent the energy density of baryon and cold dark matter respectively,  $\rho_{DE}$  is the energy density of dark energy with a dynamic EoS  $w_{DE}$ , and  $H = \dot{a}/a$  is Hubble parameter. Many interacting theoretical models have been studied (Amendola 2000; Farrar & Peebles 2004; Guo, Cai & Zhang 2005; Szydlowski 2006; Sadjadi & Alimohammadi 2006; Del Campo et al. 2006; Wei & Cai 2006; Bertolami, Gil Pedro & Le Delliou 2007; Cai & Su 2010). But the interaction term  $Q$  is still poorly known. Many phenomenological models have been put forward to solve it, such as a simple phenomenological coupling form  $Q = C\delta(a)H\rho_{DM}$  (Dalal et al. 2001; Amendola, Campos & Rosenfeld 2007; Guo, Ohta & Tsujikawa 2007; Wei 2010; Cao, Liang & Zhu 2011), where  $C$  is constant. The EoS of dark energy is needed to solve the Eq.2. In this paper we will discuss a phenomenological model with a dynamic EoS (Chevallier & Polarski 2001; Linder 2003),

$$w_{DE}(z) = w_0 + w_1 z/(1+z). \quad (3)$$

Then we calculate the evolution of energy density of DM and DE. The transition redshift is also constrained in this interacting phenomenological model (Abdel-Rahman & Riad 2007).

The structure of this paper is arranged as follows. In section 2, we will analyze the model. In section 3, we constrain model parameters using the observational data sets. In section 4, we present results. The conclusions and discussions will be given in section 5.

Send offprint requests to: F. Y. Wang(fayinwang@nju.edu.cn)

## 2. Interacting dark sector model

The interaction is between the non-baryonic dark matter and the quintessence field. The mass evolution of dark matter particles can be written as  $m = m(\Phi(a))$ , and parameterize in a function of the scale factor  $\delta(a)$  (Amendola, Campos & Rosenfeld 2007; Majerotto, Sapone & Amendola 2004; Rosenfeld 2005),

$$m(a) = m_0 e^{\int_1^a \delta(a') d \ln a'}, \quad (4)$$

where  $m_0$  is the dark matter mass today and  $\delta(a) = d \ln m / d \ln a$  represents the rate of change of the dark matter mass. We will set  $\delta(a)$  as a constant in this paper (Amendola, Campos & Rosenfeld 2007).

The evolutions of  $\rho_{DM}$  and  $\rho_{DE}$  can be expressed as

$$\dot{\rho}_{DM} + 3H\rho_{DM} - \delta H\rho_{DM} = 0, \quad (5)$$

$$\dot{\rho}_{DE} + 3H\rho_{DE}(1 + w_{DE}) + \delta H\rho_{DM} = 0. \quad (6)$$

The interacting term is  $Q = -\delta H\rho_{DM}$ . Then Eq. (5) can be solved in the assumption of a constant interaction,

$$\rho_{DM}(a) = \rho_{DM}^0 a^{-3+\delta}, \quad (7)$$

where  $\rho_{DM}^0$  is the dark matter energy density today. Substituting this solution into Eq. (6), we obtain the evolution of  $\rho_{DE}$ ,

$$\frac{d\rho_{DE}}{da} + \frac{3}{a}\rho_{DE}(1 + w_{DE}) + \delta\rho_{DM}^0 a^{-4+\delta} = 0. \quad (8)$$

Amendola et al. (2007) studied the interacting model with a EoS  $w_{DE}(z) = w_0 + w_1 z$ . But that model is not compatible with CMB data since it diverges at high redshift (Chevallier & Polarski 2001). We consider an extended parameterization of EoS as Eq.(3) to avoid this problem (Chevallier & Polarski 2001; Linder 2003). Then we obtain solution of Eq. (8) as a function of redshift  $z$ ,

$$\rho_{DE}(z) = \rho_{DE}^{NI}(z) [1 + \Theta(z, w_0, w_1, \delta)], \quad (9)$$

where

$$\rho_{DE}^{NI}(z) = \rho_{DE}^0 e^{-3w_1 z / (1+z)} (1+z)^{3(1+w_0+w_1)}. \quad (10)$$

It represents the evolution of dark energy density without interaction for this parameterization. The  $\Theta$  function is

$$\begin{aligned} \Theta(z, w_0, w_1, \delta) &= \delta e^{3w_1} (3w_1)^{-3(w_0+w_1)-\delta} \times \frac{\rho_{DM}^0}{\rho_{DE}^0} \\ &\times \Gamma(3(w_0 + w_1) + \delta, 3w_1 / (1+z), 3w_1), \end{aligned} \quad (11)$$

where  $\Gamma(a, x_0, x_1)$  is the generalized incomplete gamma function  $\Gamma(a, x_0, x_1) = \int_{x_0}^{x_1} t^{a-1} e^{-t} dt$ .

Then the Hubble parameter in this dark interaction model can be written as

$$\begin{aligned} E(z, \Omega_{DM}^0, w_0, w_1, \delta) &= [\Omega_{DM}^0 (1+z)^{3-\delta} + \Omega_B^0 (1+z)^3 \\ &+ (1 - \Omega_B^0 - \Omega_{DM}^0 - \Omega_r^0) (1+z)^{3(1+w_0+w_1)} \\ &\times e^{-3w_1 z / (1+z)} (1 + \Theta(z, w_0, w_1, \delta)) + \Omega_r^0 (1+z)^4]^{1/2}, \end{aligned} \quad (12)$$

where  $\Omega_{DM}^0$ ,  $\Omega_B^0$  and  $\Omega_r^0$  are the dark matter, the baryonic and radiation density fractions today, respectively. We adopt  $\Omega_B^0 = 0.0487 \pm 0.0006$  (Planck Collaboration et al. 2013),  $H_0 = 73.8 \pm 2.4 \text{ kms}^{-1} \text{ Mpc}^{-1}$  (Riess et al. 2011) and  $\Omega_r^0 = (\Omega_{DM}^0 + \Omega_B^0) / (1 + z_{eq})$ , where  $z_{eq}$  is the redshift when matter energy density is equal to radiation energy density.

## 3. Observational data

In order to constrain the parameters tightly, we combine SNe Ia sample, Hubble parameter data, BAO measurements and CMB observation. Each one of these data can constrain cosmological parameter compactly and consistently (Suzuki et al. 2012; Farooq & Ratra 2013; Hinshaw et al. 2013; Planck Collaboration et al. 2013).

### 3.1. SNe Ia data

SNe Ia data is the first evidence for the accelerating expansion of the universe, and it can be taken as standard candles to measure the luminosity distance. We use the latest Union 2.1 sample (Suzuki et al. 2012), which contains 580 SNe Ia in the redshift range  $0.014 < z < 1.415$ . With the measured luminosity distance  $d_L$  in units of megaparsecs, the predicted distance modulus can be given as

$$\mu = 5 \log(d_L) + 25, \quad (13)$$

where the luminosity distance is expressed as

$$d_L(z, \Omega_{DM}^0, w_0, w_1, \delta) = c \frac{(1+z)}{H_0} \int_0^z \frac{dz'}{E(z', \Omega_{DM}^0, w_0, w_1, \delta)}. \quad (14)$$

The likelihood functions can be determined from  $\chi_{SNe}^2$  distribution (Nesseris & Perivolaropoulos 2005; Wang 2012),

$$\chi_{SNe}^2 = A - \frac{B^2}{C}, \quad (15)$$

where  $A = \sum_i^{580} (\mu^{obs} - \mu^{th})^2 / \sigma_{\mu,i}^2$ ,  $B = \sum_i^{580} (\mu^{obs} - \mu^{th}) / \sigma_{\mu,i}^2$ ,  $C = \sum_i^{580} 1 / \sigma_{\mu,i}^2$ .  $\mu^{obs}$  is the observational distance modulus, and  $\sigma_{\mu,i}$  is the  $1\sigma$  uncertainty of the distance moduli.

### 3.2. Hubble parameter data

The Hubble parameter sample contains 28 data points, which cover redshift range  $0.07 \leq z \leq 2.3$ . This is the largest data set of  $H(z)$ , with nine data from Simon, Verde & Jimenez (2005), two from Stern et al. (2010), eight from Moresco et al. (2012), one from Busca et al. (2013), four from Zhang et al. (2012), three from Blake et al. (2012), and one from Chuang & Wang (2013). These data have been compiled by Farooq & Ratra (2013) (see their Table 1). The  $\chi_H^2$  is given as

$$\chi_H^2 = \sum_{i=1}^{28} \frac{[H(z_i) - H_{obs}(z_i)]^2}{\sigma_{h,i}^2}, \quad (16)$$

where theoretical  $H(z)$  can be obtained from Eq. (12),  $H_{obs}$  and  $\sigma_{h,i}$  are observed value.

### 3.3. Baryon Acoustic Oscillations

The BAO peak in galaxy correlation function is first detected in the 2dFGRS (Cole et al. 2005) and SDSS (Eisenstein et al. 2005). Now the BAO redshift covers the range  $0.1 \leq z \leq 0.73$ . The distance ratio  $d_z$  is defined as

$$d_z = \frac{r_s(z_d)}{D_V(z_{BAO})}, \quad (17)$$

where the angular diameter distance scale  $D_V$  is given by Eisenstein et al. (2005),

$$D_V(z_{BAO}) = \frac{1}{H_0} \left[ \frac{z_{BAO}}{E(z_{BAO})} \left( \int_0^{z_{BAO}} \frac{dz}{E(z)} \right)^2 \right]^{1/3}. \quad (18)$$

The comoving sound horizon at the drag epoch is  $r_s(z_d) = H_0^{-1} \int_{z_d}^{\infty} c_s(z)/E(z)dz$ . Following Eisenstein & Hu (1998), the decouple redshift is

$$z_d = \{1291(\Omega_M^0 h^2)^{0.251}/[1 + 0.659(\Omega_M^0 h^2)^{0.828}]\} \times [(1 + b_1(\Omega_B^0 h^2)^{b_2})], \quad (19)$$

with

$$b_1 = 0.313(\Omega_M^0 h^2)^{-0.419}[1 + 0.607(\Omega_M^0 h^2)^{0.674}]^{-1}, \quad (20)$$

$$b_2 = 0.238(\Omega_M^0 h^2)^{0.223}. \quad (21)$$

Here we will use the results from four data sets: 6dF Galaxy Redshift Survey measurements at efficient redshift  $z_{eff} = 0.1$  (Beutler et al. 2011), the SDSS DR7 BAO measurements at  $z_{eff} = 0.35$  (Padmanabhan et al. 2012), the BOSS DR 9 measurements at  $z_{eff} = 0.57$  (Anderson et al. 2012), and WiggleZ measurements at higher redshift  $z_{eff} = 0.44, 0.60, 0.73$  (Blake et al. 2012).

The distance ratio vector is

$$\mathbf{P}_{\text{BAO}}^{\text{obs}} = \begin{pmatrix} d_{0.1} \\ d_{0.35}^{-1} \\ d_{0.57}^{-1} \\ d_{0.44} \\ d_{0.60} \\ d_{0.73} \end{pmatrix} = \begin{pmatrix} 0.336 \\ 8.88 \\ 13.67 \\ 0.0916 \\ 0.0726 \\ 0.0592 \end{pmatrix}. \quad (22)$$

The corresponding inverse covariance matrix is

$$\mathbf{C}_{\text{BAO}}^{-1} = \begin{pmatrix} I_1 & 0 \\ 0 & I_2 \end{pmatrix}, \quad (23)$$

where

$$\mathbf{I}_1 = \begin{pmatrix} 4444.4 & 0 & 0 \\ 0 & 34.602 & 0 \\ 0 & 0 & 20.661157 \end{pmatrix}, \quad (24)$$

$$\mathbf{I}_2 = \begin{pmatrix} 24532.1 & -25137.7 & 12099.1 \\ -25137.7 & 134598.4 & -64783.9 \\ 12099.1 & -64783.9 & 128837.6 \end{pmatrix}. \quad (25)$$

The  $\chi_{\text{BAO}}^2$  value of the BAO can express as

$$\chi_{\text{BAO}}^2 = \Delta \mathbf{P}_{\text{BAO}}^{\text{T}} \mathbf{C}_{\text{BAO}}^{-1} \Delta \mathbf{P}_{\text{BAO}}, \quad (26)$$

where  $\Delta \mathbf{P}_{\text{BAO}} = \mathbf{P}_{\text{BAO}}^{\text{th}} - \mathbf{P}_{\text{BAO}}^{\text{obs}}$ .

### 3.4. CMB from WMAP 9 years

We also use the WMAP 9 years data. We use the ‘‘WMAP distance priors’’ likelihood of 3 variables: the acoustic scale  $l_a$ , the shift parameter  $R$ , and the recombination redshift  $z_*$  to constrain parameters. They can be expressed as

$$l_a = \pi \frac{\int_0^{z_*} \frac{dz}{E(z)}/H_0}{r_s(z_*)}, \quad (27)$$

$$R = \frac{\Omega_{\text{M}0}^{1/2} H_0}{c} \int_0^{z_*} \frac{dz}{E(z)}, \quad (28)$$

and the recombination redshift is given by Hu & Sugiyama (1996),

$$z_* = 1048[1 + 0.00124(\Omega_B^0 h^2)^{-0.738}(1 + g_1(\Omega_M^0 h^2)^{g_2})], \quad (29)$$

with

$$g_1 = 0.0783(\Omega_B^0 h^2)^{-0.238}(1 + 39.5(\Omega_B^0 h^2)^{0.763})^{-1}, \quad (30)$$

$$g_2 = 0.560(1 + 21.1(\Omega_B^0 h^2)^{1.81})^{-1}. \quad (31)$$

The best fitted data are given by Hinshaw et al. (2013),

$$\mathbf{P}_{\text{CMB}}^{\text{obs}} = \begin{pmatrix} l_a \\ R \\ z_* \end{pmatrix} = \begin{pmatrix} 302.40 \\ 1.7246 \\ 1090.88 \end{pmatrix}. \quad (32)$$

The corresponding inverse covariance matrix can be written as

$$\mathbf{C}_{\text{CMB}}^{-1} = \begin{pmatrix} 3.182 & 18.253 & -1.429 \\ 18.253 & 11887.879 & -193.808 \\ -1.429 & -193.808 & 4.556 \end{pmatrix}. \quad (33)$$

The  $\chi_{\text{CMB}}^2$  value of CMB is

$$\chi_{\text{CMB}}^2 = \Delta \mathbf{P}_{\text{CMB}}^{\text{T}} \mathbf{C}_{\text{CMB}}^{-1} \Delta \mathbf{P}_{\text{CMB}}, \quad (34)$$

where  $\Delta \mathbf{P}_{\text{CMB}} = \mathbf{P}_{\text{CMB}}^{\text{th}} - \mathbf{P}_{\text{CMB}}^{\text{obs}}$ .

## 4. Methods and Results

With the joint data, the total  $\chi^2$  can be expressed as

$$\chi^2(\delta, \Omega_{\text{DM}}, w_0, w_1) = \chi_{\text{SNe}}^2 + \chi_H^2 + \chi_{\text{BAO}}^2 + \chi_{\text{CMB}}^2. \quad (35)$$

The model parameters can be determined by computing the  $\chi^2$  distribution. First, we calculate the minimum value of the total  $\chi^2/dof = 0.990$  from simultaneous fitting. Then, we calculate the inverse covariance matrix to give out the best-fitted value's  $1\sigma$  uncertainty  $\delta = -0.022 \pm 0.006$ ,  $\Omega_{\text{DM}}^0 = 0.213 \pm 0.008$ ,  $w_0 = -1.210 \pm 0.033$  and  $w_1 = 0.872 \pm 0.072$ .

In order to obtain the contour plot, we marginalize over other two parameters to get a new  $\chi^2$  function depending on two left parameters,

$$\chi^2(\delta, \Omega_{\text{DM}}) = \frac{1}{\Psi} \int_{w_0 - \sigma_{w_0}}^{w_0 + \sigma_{w_0}} \int_{w_1 - \sigma_{w_1}}^{w_1 + \sigma_{w_1}} \chi^2(\delta, \Omega_{\text{DM}}, w_0, w_1) dw_0 dw_1, \quad (36)$$

where  $\Psi$  is the normalization factor to make the  $\chi^2$  have the same minimum value as  $\chi^2$ . Then use  $\chi^2$  to give the  $\delta - \Omega_{\text{DM}}$  2D marginalized regions with different colors representing  $1\sigma$  and  $2\sigma$  regions. Figure 1 shows the  $\delta - \Omega_{\text{DM}}$  contours with different data combinations: SNe (gray and light gray contours), SNe + BAO (red and pink contours), SNe + CMB (blue and light purple contours), CMB + BAO + H(z) (Orange and yellow contours) and the full data sets (black and cyan contours). This figure shows that the BAO data can set tight constraint on  $\Omega_{\text{DM}}$ , while CMB can set tighter constraint on  $\delta$  and  $\Omega_{\text{DM}}$ . From Figure 1, we find that there is a tension between the SNe data and other data sets. The tension has been investigated by Nesseris & Perivolaropoulos (2005) and Wei (2010).

In order to test the reliability of our method, we also show  $w_0 - w_1$  contours from SNe+BAO+CMB without considering coupling ( $\delta = 0$ ) with  $1\sigma$  in black region and  $2\sigma$  in grey region contours, which is presented in the left panel of Figure 2. We can see that the our result is consistent with that of WMAP team by comparing this figure with the Figure 10 of Hinshaw et al.

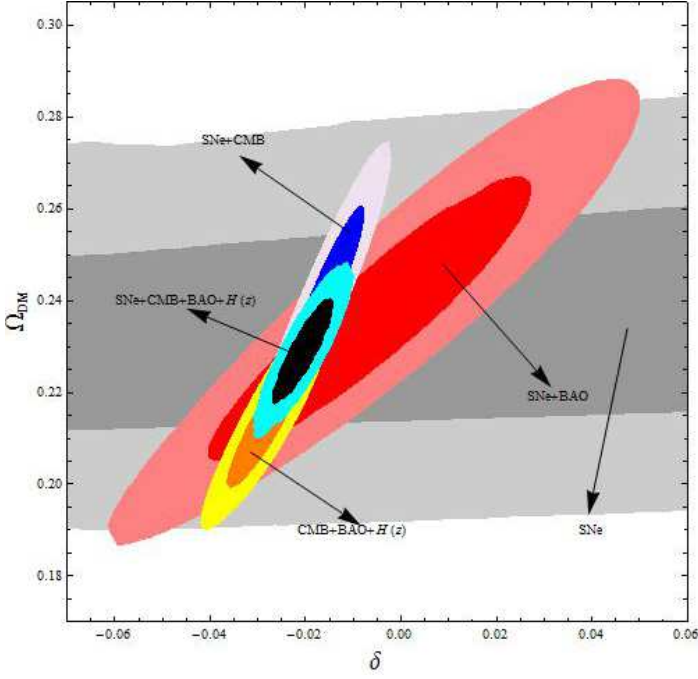


Fig. 1: The  $\delta - \Omega_{DM}$  contours with different data combinations: SNe (gray and light gray contours), SNe + BAO (red and pink contours), SNe + CMB (blue and light purple contours), CMB + BAO +  $H(z)$  (orange and yellow contours) and SNe + CMB + BAO +  $H(z)$  (black and cyan contours). The central regions and the vicinity regions represent  $1\sigma$  contours and  $2\sigma$  contours, respectively.

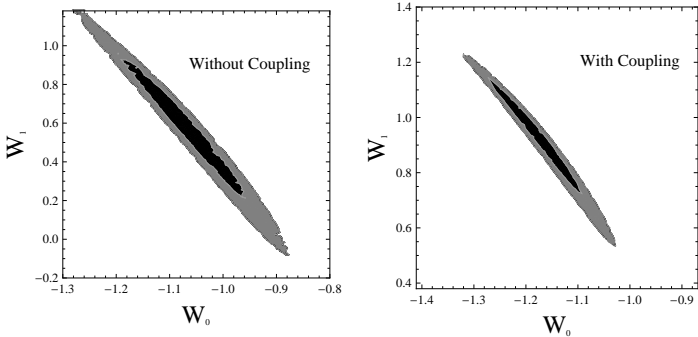


Fig. 2: The black and grey regions are  $1\sigma$  contours and  $2\sigma$  contours, respectively. The left panel is  $w_0$  vs  $w_1$  without coupling, and the right panel is  $w_0$  vs  $w_1$  with coupling in our model.

(2013). The right panel of Figure 2 shows the  $w_0 - w_1$  contours with coupling. We show  $\delta - w_0$  and  $\Omega_{DM} - w_1$  contours in Figure 3 and  $\delta - w_1$  and  $\Omega_{DM} - w_0$  contours in Figure 4, respectively.

From the best-fitted parameters, the energy density evolution of DM and DE can be calculated. The ratio of DM density and DE density is

$$\rho_{DM}/\rho_{DE} = \rho_{DM}^0 a^{-3+\delta} / (\rho_{DE}^0(z) [1 + \Theta(z, w_0, w_1, \delta)]). \quad (37)$$

Figure 5 shows the evolution of  $\rho_{DM}/\rho_{DE}$  as a function of scale factor  $a$  with best-fitted parameters. The gray region is the  $1\sigma$

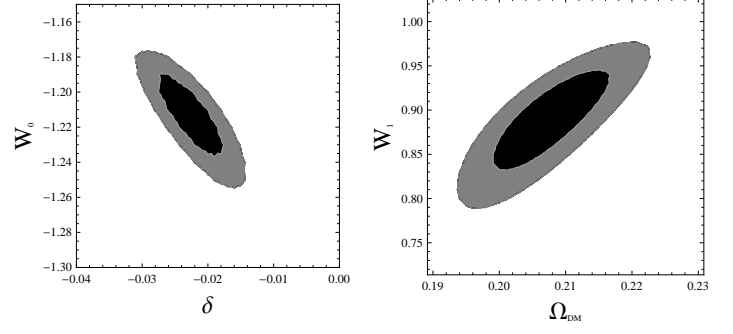


Fig. 3: The black and grey regions are  $1\sigma$  contours and  $2\sigma$  contours, respectively. The left panel is  $\delta$  vs  $w_0$ , and the right panel is  $\Omega_{DM}$  vs  $w_1$ .

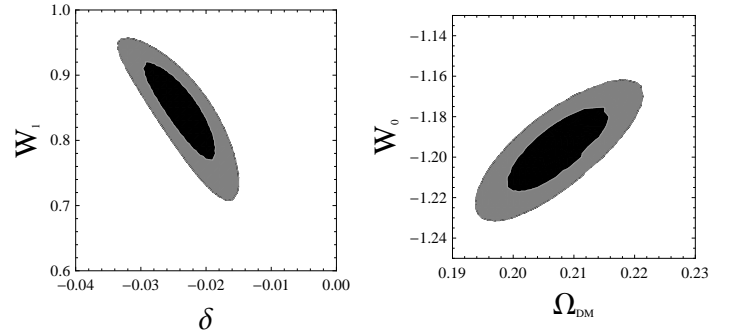


Fig. 4: The black and grey regions are  $1\sigma$  contours and  $2\sigma$  contours, respectively. The left panel is  $\delta$  vs  $w_1$ , and the right panel is  $\Omega_{DM}$  vs  $w_0$ .

uncertainty in this model, and the black one is for the  $\Lambda$ CDM case. In our model,  $\delta < 0$  means that the energy transfers from dark matter to dark energy, which is consisted with Dalal et al. (2001) and Guo, Ohta & Tsujikawa (2007). Nevertheless, the energy density proportion evolves slower than that in  $\Lambda$ CDM case within  $1\sigma$  uncertainties when  $a < 0.5$ , which means that our model can help to relieve the coincidence problem significantly.

The evolution of DE density plays an important role in solving the coincidence problem. Using Eq.(9) we can compute the DE evolution, which is shown in Figure 6. The gray region aloft the black line shows that the DE density is decreasing within  $1\sigma$  when  $a < 0.5$ , which can make the evolution of  $\rho_{DM}/\rho_{DE}$  slower, resulting in a good solution to the coincidence problem. However, the DE density evolves quite quickly in the very early stage of the universe when  $a < 0.3$ . The main reason is that DM mass transfer rate  $\delta$  is assumed as a constant in our model.

Our universe is undergoing an accelerating expansion now. But in the very early time, the universe was decelerating. So the evolution of deceleration parameter  $q(z)$  is important, especially when  $q(z_{tr}) = 0$ ,  $z_{tr}$  is the transition redshift.  $q(z)$  can be expressed as

$$q = -\frac{a\ddot{a}}{\dot{a}^2} = -1 + \frac{1+z}{2H(z)^2} \frac{dH(z)^2}{dz}. \quad (38)$$

After substituting the best-fitted parameters and their uncertainties in Eq. (38), we obtain  $z_{tr} = 0.63 \pm 0.07$ . This value is a lit-

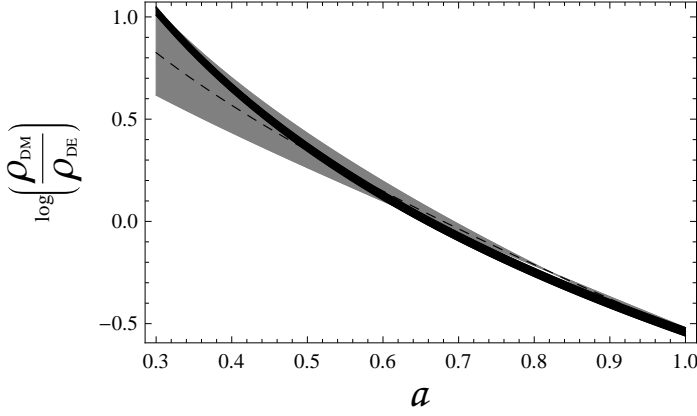


Fig. 5: The evolution of  $\rho_{DM}/\rho_{DE}$  as a function of scale factor  $a(z)$ . The dashed line is the interacting model with best-fitted parameters, and the gray region is the  $1\sigma$  uncertainties. The black region represents the  $\Lambda$ CDM with uncertainties.

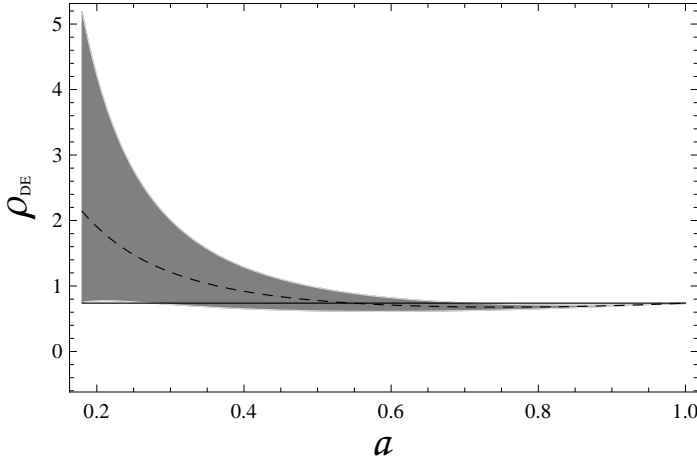


Fig. 6: The evolution of  $\rho_{DE}$  as a function of scale factor  $a(z)$ . The dashed line is the interacting model with best-fitted parameters, and the gray region is the  $1\sigma$  uncertainties. The black line represent the  $\Lambda$ CDM case.

tle bigger than those of Wang & Dai (2006), Wang, Dai & Zhu (2007) and Abdel-Rahman & Riad (2007) in  $\Lambda$ CDM. The reason is that there exists an energy transfer from DM to DE in our model. The DM density decreases quicker than that in the  $\Lambda$ CDM, while the DE density is decreasing much quicker in early times. So a higher transition redshift is needed for DE to oppose gravitation.

## 5. Conclusions and Discussions

In this paper, we use the Union 2.1 SNe Ia, CMB from WMAP 9 years, BAO observation data from 6dFGRS, SDSS DR7, BOSS DR9, WiggleZ and the latest Hubble parameter data to test the phenomenological interacting dark sector scenario with a dynamic equation of state  $w_{DE}(z) = w_0 + w_1 z / (1 + z)$ . We give more stringent constraints on the phenomenological model parameters:  $\delta = -0.022 \pm 0.006$ ,  $\Omega_{DM}^0 = 0.213 \pm 0.008$ ,  $w_0 = -1.210 \pm 0.033$  and  $w_1 = 0.872 \pm 0.072$  with  $\chi_{min}^2/dof = 0.990$ . From the contours using different data combination in Figure 1,

we find that the SNe Ia are in tension with the CMB, BAO and Hubble parameter data.

Our phenomenological scenario gives  $\delta < 0$  at  $1\sigma$  confidence level, which is consistent with Dalal et al. (2001) and Guo, Ohta & Tsujikawa (2007). It indicates that the energy transfers from dark matter to dark energy. But the evolution of  $\rho_{DM}/\rho_{DE}$  is slower than that in  $\Lambda$ CDM within  $1\sigma$  uncertainties, due to the  $\rho_{DE}$  decreases with scale factor  $a$ . So our model gives out a good approach to solve the coincidence problem.

The DE density evolves quickly in very early epoch of the universe, which is shown in Figure 6. The main reason is that the value of  $\delta$  is assumed to be constant in our model. In real case, the DM mass transfer rate  $\delta(a)$  should be varied. We also derive the transition redshift  $z_{tr} = 0.63 \pm 0.07$  in this model. Due to the interaction between DE and DM, the DE density decreases very quick in early times, so a higher transition redshift is needed to resist gravitation.

## Acknowledgments

We thank the anonymous referee for helpful comments and suggestions that have helped us improve our manuscript. This work is supported by the National Basic Research Program of China (973 Program, grant 2014CB845800) and the National Natural Science Foundation of China (grants 11373022, 11103007, 11033002 and J1210039).

## References

- Abdel-Rahman, A.-M. M. & Riad, I. F., 2007, AJ, 134, 1391
- Amendola, L., 2000, PhRvD, 62, 043511
- Amendola, L., Campos, G. C. & Rosenfeld, R., 2007, PhRvD, 75, 083506
- Anderson, L., et al., 2012, MNRAS, 427, 3435
- Armendariz-Picon, C., Mukhanov, V. & Steinhardt, P. J., 2001, PhRvD, 63, 103510
- Bertolami, O., Gil Pedro, F. & Le Delliou, M., 2007, PhLB, 654, 165
- Beutler, F., et al., 2011, MNRAS, 416, 3017
- Blake, C., et al., 2012, MNRAS, 425, 405
- Busca, N. G., et al., 2013, A&A, 552, A96
- Cai, R.-G. & Su, Q., 2010, PhRvD, 81, 103514
- Caldwell, R. R., 2002, PhLB, 545, 23
- Cao, S., Liang, N. & Zhu, Z.-H., 2011, IJMPD, 22, 14
- Chevallier, M. & Polarski, D., 2001, IJMPD, 10, 213
- Chuang, C.-H. & Wang, Y., 2013, MNRAS, 1955
- Cole, S., et al., 2005, MNRAS, 362, 505
- Dalal, N., Abazajian, K., Jenkins, E. & Manohar, A. V., 2001, PhRvL, 87, 141302
- Del Campo, S., Herrera, R., Olivares, G. & Pavón, D., 2006, PhRvD, 74, 023501
- Eisenstein, D. J. & Hu W., 1998, ApJ, 496, 605
- Eisenstein, D. J., et al., 2005, ApJ, 633, 560
- Farooq, O. & Ratra, B., 2013, ApJ, 766, L7
- Farrar, G. R. & Peebles, P. J. E., 2004, ApJ, 604, 1
- Feng, B., Wang, X. & Zhang, X., 2005, PhLB, 607, 35
- Guo, Z.-K., Cai, R.-G. & Zhang Y.-Z., 2005, JCAP, 5, 2
- Guo, Z.-K., Ohta, N. & Tsujikawa, S., 2007, PhRvD, 76, 023508
- Hinshaw, G., et al., 2013, ApJS, 208, 19
- Hu, W. & Sugiyama, N., 1996, ApJ, 471, 542
- Linder, E. V., 2003, PhRvL, 90, 091301
- Majerotto, E., Sapone, D. & Amendola, L., 2004, astro, arXiv:astro-ph/0410543
- Moresco, M., et al., 2012, JCAP, 8, 6
- Nesseris, S. & Perivolaropoulos, L., 2005, PhRvD, 72, 123519
- Padmanabhan, N., Xu, X., Eisenstein, D. J., Scalzo, R., Cuesta, A. J., Mehta, K. T. & Kazin, E., 2012, MNRAS, 427, 2132
- Percival, W. J., et al., 2010, MNRAS, 401, 2148
- Perlmutter, S., et al., 1999, ApJ, 517, 565
- Planck Collaboration, et al., 2013, arXiv:1303.5076
- Ratra, B. & Peebles, P. J. E., 1988, PhRvD, 37, 3406
- Riess, A. G., et al., 1998, AJ, 116, 1009
- Riess, A. G., et al., 2011, ApJ, 730, 119
- Rosenfeld, R., 2005, PhLB, 624, 158
- Sadjadi, H. M. & Alimohammadi, M., 2006, PhRvD, 74, 103007

- Simon, J., Verde, L. & Jimenez, R., 2005, *PhRvD*, 71, 123001  
Stern, D., Jimenez, R., Verde, L., Kamionkowski, M. & Stanford, S. A., 2010, *JCAP*, 2, 8  
Suzuki, N., et al., 2012, *ApJ*, 746, 85  
Szydlowski, M., 2006, *PhLB*, 632, 1  
Wang, F. Y., 2012, *A&A*, 543, A91  
Wang, F. Y. & Dai, Z. G., 2006, *MNRAS*, 368, 371  
Wang, F. Y., Dai, Z. G. & Zhu, Z. H., 2007, *ApJ*, 667, 1  
Wei, H., 2010, *PhLB*, 687, 286  
Wei, H., 2010, *PhLB*, 691, 173  
Wei, H. & Cai, R.-G., 2006, *PhRvD*, 73, 083002  
Zhang, C., Zhang, H., Yuan, S., Zhang, T.-J. & Sun, Y.-C., 2012, *arXiv:1207.4541*